Energy dependence of μ^- transfer rate to Oxygen

FAMU experiment for the measurement of the HFS

D. Bakalov, M.N. Stoilov & P. Danev for the FAMU collaboration

Institute for Nuclear Research and Nuclear Energy

Bulgarian Academy of Sciences

Introduction

Muonic hydrogen $p\mu$ lifetime allows precision spectroscopy.
– The ground-state hyperfine splitting of $p\mu$, $\Delta E^{\rm hfs} \sim 0.182$ eV, is in the infra-red optical range and enables laser spectroscopy.
– A number of experimental proposals for the measurement of $\Delta E^{\rm hfs}$ have been put forward in recent years, stimulated by the need of new data on the proton electromagnetic structure that had become an issue with the proton charge radius determination from the Lamb shift in muonic hydrogen [Pohl et al.,2010].
– In all these proposals $p\mu$ is excited from the ground singlet to the triplet state with a laser, tunable around the resonance frequency $\Delta E^{\rm hfs}/h \sim 44$ THz; the experimental methods differ by the signature used to detect the laser-induced transitions.

FAMU experimental method

1. The $p\mu$'s in $1s(\uparrow\downarrow)$ state propagate in a H_2 and O_2 gas mixture.
2. Part of the $p\mu$'s are excited to the $1s(\uparrow\uparrow)$ state with laser pulse.
3. In collisions with H_2 the $p\mu$'s are de-excited back to $(\uparrow\downarrow)$ state. These atoms carry away nearly 2/3 of the released energy $E^{\rm hfs}(\sim 0.12$ eV) as additional kinetic energy.
4. In collisions of $p\mu$ with O_2 the muon is transferred to μO^*.
– The rate of muon transfer to oxygen from accelerated $p\mu$'s exceeds the rate from thermal $p\mu$'s.
5. The formation of μO^* is signalled by the emission of characteristic X-rays during relaxation.

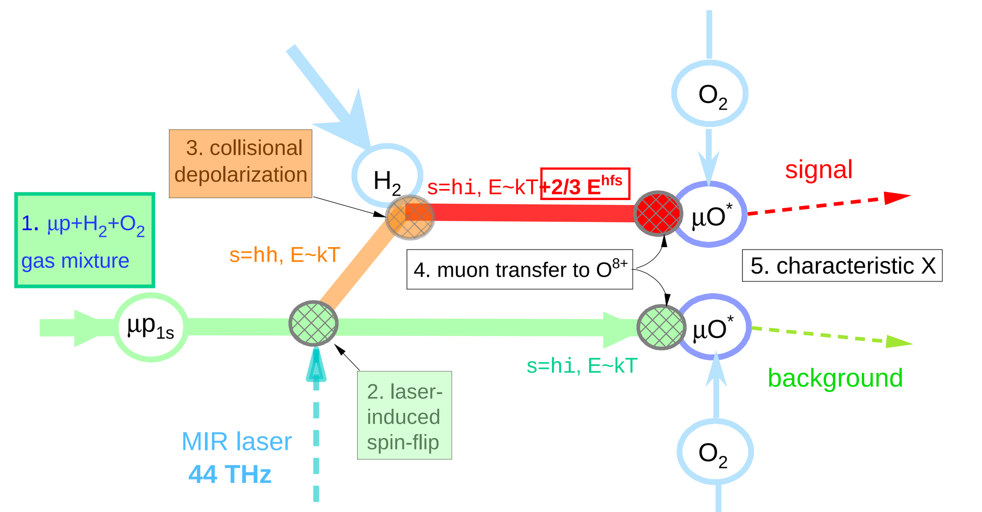

6. Observable: time distribution characteristic of X-rays.
7. The fast muon transfer from accelerated μp perturbs the exponential background from thermal μp's.

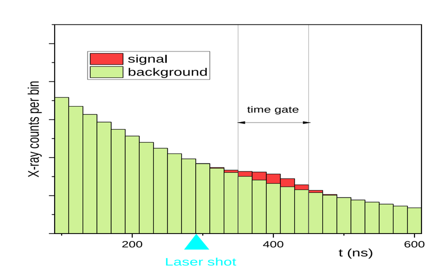

– Signal: the difference of the time distributions with and without laser pulse.
– The more spin-flipped μp's, the stronger the signal
– Maximal signal – at laser frequency in resonance with the hyperfine splitting $\Delta E^{\rm hfs}$.

– The efficiency of the method: determined by the collision energy dependence $\lambda_{p{\rm O}}(E)$ of the rate of muon transfer

$$(p\mu)_{1s} + O \to (O\mu)^* + p.$$

– The hydrogen-oxygen mixture – selected because of indications of a sharp raise of $\lambda_{p{\rm O}}(E)$ at thermal and near epithermal energies [Werthmüller, 1998; Dupays, 2004; Le&Lin, 2005].
– Accurate quantitative experimental verification needed.

Experimental determination of $\lambda_{p{\rm O}}({\rm E})$

– Temperature dependence $\Lambda_{p{\rm O}}(T)$ of the rate of muon transfer:

$$\Lambda_{p{\rm O}}(T) = \int dE\, \lambda_{p{\rm O}}(E)\, f(E;T) \qquad (1)$$

with $f(E;T)$ – the energy distribution of μp. In thermal equilibrium this is the Maxwell-Boltzmann distribution

$$f(E;T) = f_{\rm MB}(E;T) \sim {\rm const}\,\sqrt{E}\exp(-E/kT).$$

Table 1: FAMU data

k	T_k	Λ_k	$\delta\Lambda_k$
1	70	2.67	0.51
2	80	2.96	0.38
3	104	3.07	0.30
4	153	5.20	0.34
5	201	6.48	0.35
6	240	8.03	0.38
7	272	8.18	0.41
8	300	8.79	0.43
9	323	8.88	0.91
10	336	9.37	1.07

– $\Lambda_k = \Lambda_{p{\rm O}}(T_k)$ (normalized to LHD, in units 10^{10} s^{-1}), measured at 10 temperatures in the range 70 K$<T<$336 K, in fully thermalized gas.
– Inverse Laplace transform: inapplicable
– Computational method: probing test functions $\lambda_{p{\rm O}}(E;\{p\})$, for which $\Lambda_{p{\rm O}}(T;\{p\})$, calculated with Eq. (1) gives best fit of the data.

Fits with unconstrained test functions

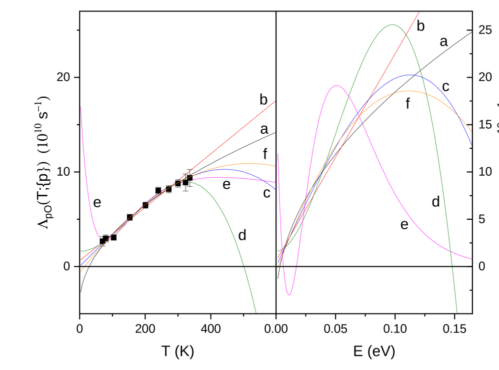

(a) $a_0 + a_1\sqrt{E}$;
(b) $a_0 + a_1 E$;
(c) $a_0 E + a_1 E^3$;
(d) $a_0 + a_1 E^2 + a_2 E^3$;
(e) $(a_0 + a_1 E + a_2 E^2)e^{-E/e_1}$;
(f) $a_0 + a_1 E + a_2 E^2$.

Unconstrained test functions reproduce the data well (low χ^2), but diverge outside the range of investigated temperatures, and lead to unphysical values and wrong asymptotics.

Constraints on the test functions

C1 - Non-negativity: $\lambda(E;\{p\}) \geq 0$ for all $E \geq 0$.
C2 - Moderate growth to secure convergence of (1).
C3 - Wigner threshold law: $\lambda_0 = \lambda(0;\{p\}) > 0$, $0 \leq d\lambda(E;\{p\})/dE \ll \lambda_0/E_0$ for $E < E_0$, $E_0 \sim 10^{-3}$ eV
C4 - Stability: No qualitative changes if fitting data subsets

Truncated polynomials

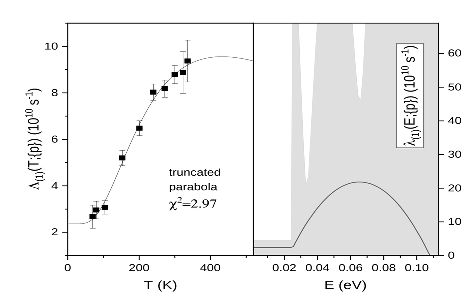

$\lambda(E) = \max(p_0 + p_1 E + p_2 E^2, 0)$
Shadowed zone: the mean prediction band (MPB) for 95% confidence level.
👍 C1 and C2 satisfied.
👎 Unacceptably broad MPB.

Step functions

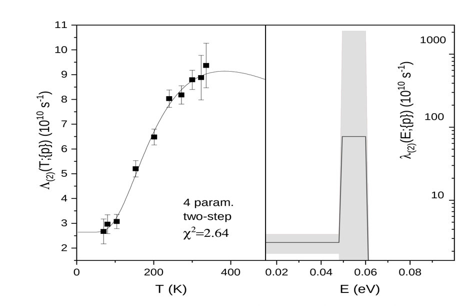

Shadowed zone: the mean prediction band (MPB) for 95% confidence level.
👍 C1 and C2 satisfied.
👎 Unacceptably broad MPB.
👎 C4: lack of stability

Large MPB – related to discontinuities of the test function

Piece-wise linear test functions

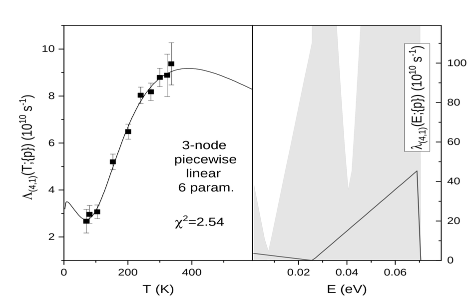

3-node, 0 for $E > 70$ meV
Shadowed: (MPB) for 95% CL.
👍 C1 satisfied.
👎 C3 not satisfied.
👎 Unacceptably broad MPB.

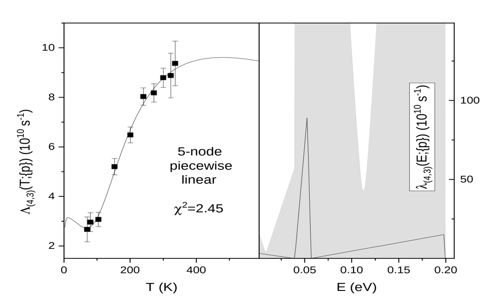

5-node, 0 for $E > 0.2$ eV
Shadowed: (MPB) for 95% CL.
👍 C1 satisfied.
👎 C3 not satisfied.
👎 Unacceptably broad MPB.
👎 C4: lack of stability

– Large MPB – related to discontinuities of the test function
– To avoid this, consider spline test function

Cubic spline test functions

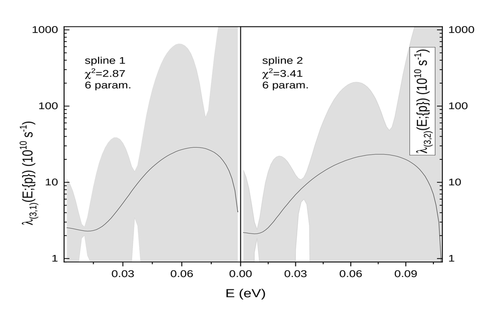

Best 3-node splines
Shadowed zone: MPB for 95% confidence level.
👍 C1 – C2 satisfied.
👍 Fairly acceptable MPB.

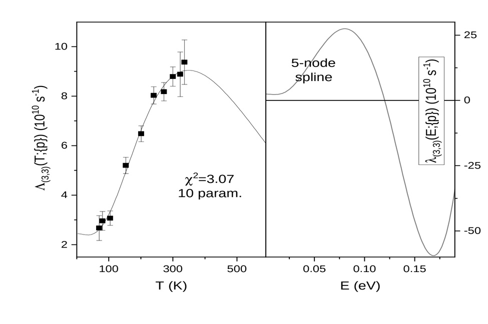

5-node spline, 0 for $E > 20$ meV
👍 Narrower MPB, but...
(#parameters)=2×(#nodes)
⇒ Oscillations for ≥ 4 nodes
👎 C1 – not satisfied.

👎 Major flaw of piece-wise test functions: large MP bands
👎 Instability of fits with only few degrees of freedom
⇒ need to use of flexible few-parameter smooth test functions

C^∞ test functions

Type 1: Gaussian-like behavior at large E

$$\lambda_{(5)}(E;\{p\}) = \Big(\sum_{k=1}^{N} p_k E^{\alpha_k}\Big)\exp(-(E-p_{N+1})^2/p_{N+2}^2) + p_{N+3},$$

Type 2: Exponential behavior at large E

$$\lambda_{(6)}(E;\{p\}) = \Big(\sum_{k=1}^{N} p_k E^{\alpha_k}\Big)\exp(-E/p_{N+1}) + p_{N+2}$$

Test functions of type 1

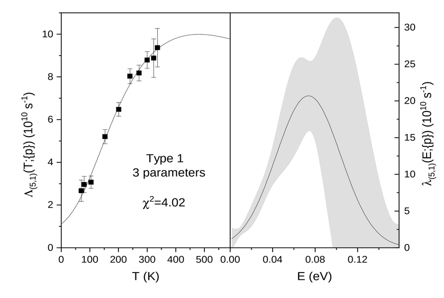

Simplest case: $N=1$, $\alpha_1 = 0$
👍 Narrow MPB for $E < 80$meV
👍 C1, C2, C4 – satisfied
👍 C3 – approx. satisfied
👍 Good $\chi^2/n.d.f = 0.57$.

For $N=2$ the following 4-parameter modification is used:
$\lambda_{5*}(E;\{p\}) = \lambda_5(E;\{p\}) - d\lambda_5(0;\{p\})/dE - d^2\lambda_5(0;\{p\})/dE^2$
to better comply with Wigner law (C3).

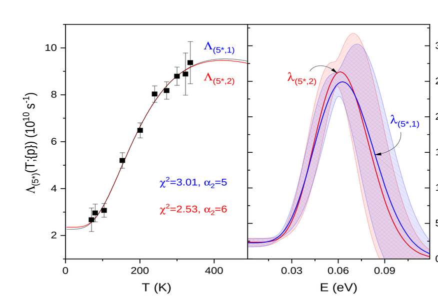

$\lambda_{5*}(E;\{p\})$ with $N=2, \alpha_1 = 0$
👍 Narrow MPB for $E < 75$meV
👍 All C1–C4 satisfied
👍 Good values of $\chi^2/n.d.f$
C3 not satisfied for $alpha_2 \geq 8$
Unstable for $N > 2$ or $p_{N+3} \neq 0$.

Test functions of type 2

$\lambda_{6*}(E;\{p\}) = \lambda_6(E;\{p\}) - d\lambda_6(0;\{p\})/dE - d^2\lambda_6(0;\{p\})/dE^2$

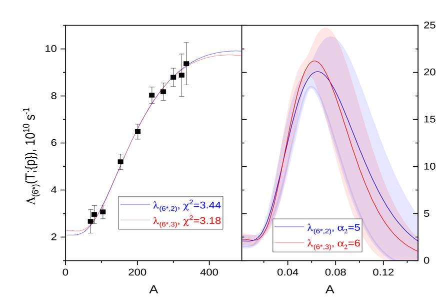

3 parameters, $N=2, \alpha_1 = 0$
👍 Narrow MPB for $E < 80$meV
👍 C1–C4 – satisfied
👍 Good $\chi^2/n.d.f = 0.57$.
C3 not satisfied for $\alpha_2 \geq 7$

Best fit

Selected 7 fits of various shape with lowest χ^2, satisfying C1-C4
Mean uncertainty band (shadowed): the envelope of the 7 fits
Best fit $\lambda_*(E)$ (thick line): the median of the envelope
$\lambda_{\rm best}(E) \approx c_1\lambda_{(5,1)}(E) + c_2\lambda_{(5*,1)}(E)$, $c_1 = 0.5771$, $c_2 = 0.4281$

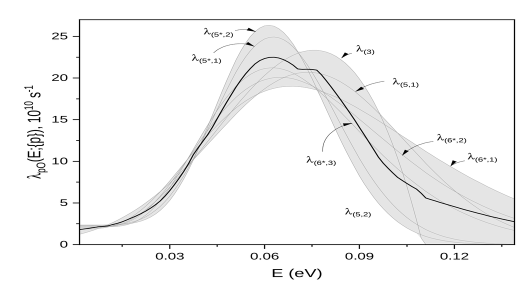

Model uncertainty (MU): envelope half-width
MU $\lesssim 20\%$ for $E < 80$meV
MU $\lesssim 60\%$ for $E < 0.1$eV

Comparison with theory and experiment

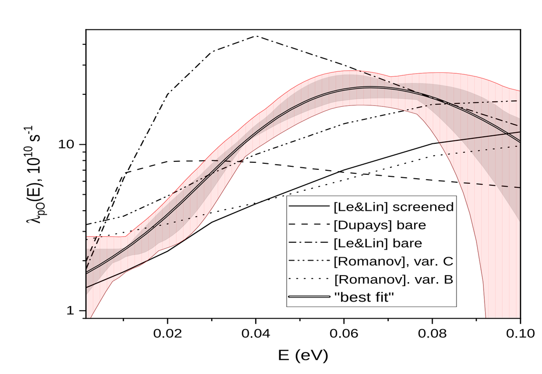

– Qualitative agreement
Peak values – between bare and screened O
Quantitatively does not confirm any computation
Nearest: Romanov (2022)

Best fit of the experimental results, present work (thick), model (gray) and statistical CL95% (pink) uncertainties, and computational results.

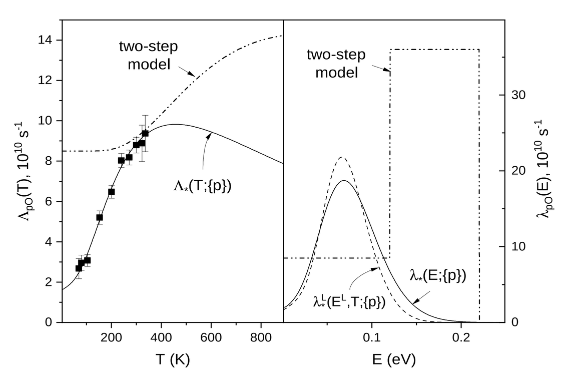

– [Werthmüller,98]: the only experimental data on $\lambda_{p{\rm O}}(E)$. The focus is on epithermal μ-transfer
– The 2-step model is inconsistent in the energy range $E < 0.1$ eV.

Summary and conclusions

1. The results reveal a raise by an order of magnitude of the muon transfer rate to oxygen with energy from $E \sim 10$ meV to $E \sim 70$ meV, and confirm the efficiency of the FAMU method.

2. The knowledge of the detailed energy dependence of $\lambda_{p{\rm O}}(E)$ provides a tool for modeling of the experiment and optimizing the experimental conditions for maximal efficiency.

3. The results set a reliable benchmark for computations of charge exchange and other low energy inelastic processes with exotic atoms.

The authors acknowledge the support of FNI Grant KP-06-N58/5.